Nucleic Acids Research, 1995, Vol. 23, No. 17 3457–3464

Repair of plasmid and genomic DNA in a *rad7Δ* mutant of yeast

James P. Mueller and Michael J. Smerdon*

Department of Biochemistry and Biophysics, Washington State University, Pullman, WA 99164-4660, USA

Received May 31, 1995; Revised and Accepted July 25, 1995

ABSTRACT

Repair of UV-induced cyclobutane pyrimidine dimers (CPDs) was examined in a yeast plasmid of known chromatin structure and in genomic DNA in a radiation-sensitive deletion mutant of yeast, *rad7Δ*, and its isogenic wild-type strain. A whole plasmid repair assay revealed that only ~50% of the CPDs in plasmid DNA are repaired after 6 h in this mutant, compared with almost 90% repaired in wild-type. Using a site-specific repair assay on 44 individual CPD sites within the plasmid we found that repair in the *rad7Δ* mutant occurred primarily in the transcribed regions of each strand of the plasmid, however, the rate of repair at nearly all sites measured was less than in the wild-type. There was no apparent correlation between repair rate and nucleosome position. In addition, ~55% of the CPDs in genomic DNA of the mutant are repaired during the 6 h period, compared with >80% in the wild-type.

INTRODUCTION

DNA repair is important for the prevention of mutagenesis and cancer (1,2). There are several mechanisms in the cell involved in removal of DNA damage, one of which is nucleotide excision repair (NER). This mechanism recognizes and removes a wide variety of bulky DNA lesions, including stable photoproducts induced by UV light. In 1987 transcription repair coupling, or the preferential repair of the transcribed strand of an active gene, was first reported in Chinese hamster ovary and human cells (3). It has since been found in yeast, both in plasmid DNA (4) and genomic DNA (5), and in *Escherichia coli* (6). In *E.coli* a protein involved in transcription repair coupling is Mfd (7). In eukaryotes the factor (or factors) responsible for this phenomenon is still unknown. However, it was recently reported that *RAD26* (the yeast homolog of human *ERCC6*, the Cockayne syndrome complementation group B gene) may be involved (8).

Of the seven essential genes for NER in yeast the roles of six have been elucidated. The genes *RAD1* and *RAD10* encode for proteins that act as a complex *in vivo* to make an incision on one side of the lesion (9–11), while the *RAD2* gene product makes an incision on the other side (12). The Rad3 protein is part of RNA polymerase II transcription factor Tfb (the yeast equivalent of TFIIH) (13). The Rad25 protein appears to interact with Tfb (13), though its role in transcription seems to be separate from its role in NER (14). Both Rad3 and Rad25 have ATPase and helicase activity (14–16). The role of the Rad3 protein might be in damage recognition, since its ATPase and helicase activities are blocked by DNA damage (17,18) and it preferentially binds to UV-damaged DNA (19). The *RAD14* gene product preferentially binds UV-damaged DNA and may be a damage recognition protein (20). The last protein essential for NER in yeast, encoded by *RAD4*, has an unknown role to date.

There are several other gene products involved in, but not essential for, NER in yeast. Among these is the product of the *RAD7* gene (21–23). Transcription of *RAD7* is inducible by UV light (4- to 6-fold) and increases 15-fold during sporulation (24). The protein has a highly hydrophilic region near the N-terminus, a hydrophobic region near the C-terminus and may possibly interact with the Rad23 protein (25). The exact role for this protein in NER is unclear. There are indications, however, that Rad7 protein is involved in allowing non-transcribed regions of the yeast genome to become accessible to repair (26,27). Both Waters *et al.* (27) and Verhage *et al.* (26) found that the non-transcribed *HMLα* locus was not repaired in a *rad7Δ* mutant, though the transcribed *MATα* locus was repaired. Verhage *et al.* (26) further showed that a *rad7Δ* mutant did not repair the non-transcribed strand of the *RPB2* gene. It has been proposed that the Rad7 protein could be involved in assembly of the repair complex (28).

Plasmid TRURAP is a yeast replicating plasmid 2619 bp in length (29). It has 14 precisely positioned nucleosomes (Fig. 1, outside ring), two of which are unstable during incubation in water (30) (Fig. 1, shaded circles). Surprisingly for such a small plasmid, five different transcripts are made (30) (Fig. 1, dashed lines). Only one of these is believed to encode a functional protein (i.e. the *URA3* mRNA); the others appear to encode nonsense mRNAs (30).

In this report we have investigated the role of the Rad7 protein in repair of TRURAP using a *rad7Δ* mutant and its isogenic wild-type strain. We examined repair in both transcribed and non-transcribed regions of this plasmid, as well as within nucleosome and non-nucleosome 'gaps'. This was done using a site-specific repair assay developed previously (4). We found that the *rad7Δ* mutant removed ~50% of the CPDs induced in TRURAP by 6 h after UV irradiation and those lesions removed lay primarily in transcriptionally active DNA. The rate of removal

* To whom correspondence should be addressed

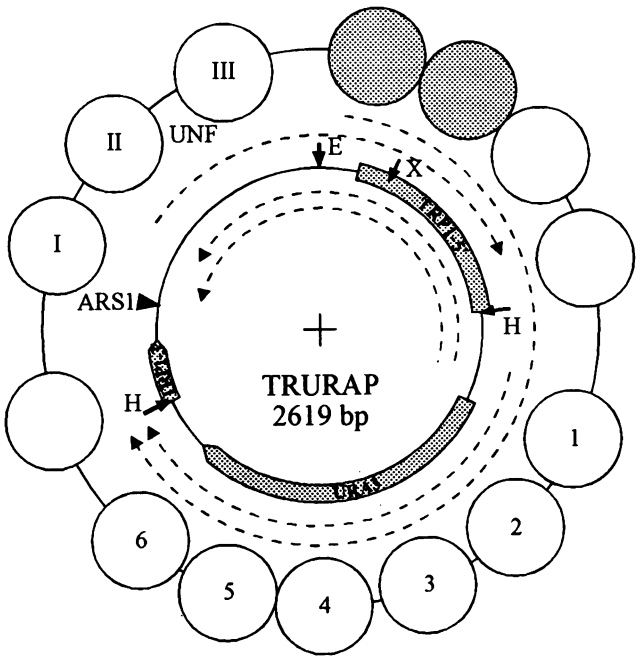

Figure 1. Plasmid TRURAP. This yeast plasmid was constructed by inserting a 1165 bp *Hin*dIII fragment encoding the *URA3* gene into the *Hin*dIII site of the TRP1ARS1 circle (29). The nucleosome positions (circles lying on the outer ring) were characterized by Thoma (29) and two nucleosomes (shaded) were found to be unstable in water (30). UNF (for unknown function) nucleosomes are now known to lie over the 5′ portion of another gene, *GAL3* (47). The locations and directions of the transcripts (dashed lines with arrow heads) were determined by Bedoyan *et al.* (30). Shaded blocks on the inner ring denote positions and direction of transcription of the *URA3* gene and the interrupted *TRP1* gene. The origin of replication, *ARS1*, is designated by the black arrowhead. Restriction sites (short arrows) are *Eco*RI (E), *Xba*I (X) and *Hin*dIII (H).

of CPDs was slower than that of wild-type at almost all sites measured in TRURAP. A similar reduction in the overall rate of removal of CPDs was observed for the genome of the *rad7*Δ mutant.

MATERIALS AND METHODS

Media and strains

The medium used in all experiments was SDM,H,W synthetic dextrose medium (2% dextrose, 0.67% yeast nitrogen base without amino acids; Difco) supplemented with histidine (20 μg/ml; Sigma) and tryptophan (40 μg/ml; Sigma) (31). Strain FTY23 is *RAD*$^+$ (MATα, *his3-1*, *trp1*, *ura3-52*::*URA3*, *gal2*, *gal10*, *cir*^{o}) and strain JMY6-7 (MATα, *his3-1*, *trp1*, *ura3-52*::*URA3*, *gal2*, *gal10*, *cir*^{o}, *rad7*Δ) is the *rad7*Δ isogenic mutant constructed for this study (see below). Strain JMY1-1 (MATa, *his3-D1*, *trp1-289*, *ura3-52*::*URA3*, *rad1*Δ) is a non-isogenic strain used as a negative control.

Construction of an isogenic *rad* mutant

To construct the isogenic mutant strain plasmid pR7.2 (kindly provided by Dr Louise Prakash, University of Texas,Galveston, TX) was cut with *Eco*RI to release a fragment containing the *URA3* gene flanked by identical *hisG* sequences which were, in turn, flanked by the 5′ and 3′ regions of the *RAD7* gene. This was transformed into yeast strain Sc3 (parent of FTY23, missing TRURAP) as described (32) with single-stranded calf thymus DNA as the carrier DNA (33) under uracil selection. A major portion of the ORF of the *RAD7* gene is deleted (nucleotides +121 to +1454, termination codon at +1696; L.Prakash, personal communication). Clones sensitive to UV were mated to a known *rad7* strain to ensure that the correct gene had been removed. The *URA3* marker was removed by growth on 5-fluoroorotic acid (34). Plasmid TRURAP was then introduced as described above for plasmid pR7.2.

Cell growth and UV irradiation

For all experiments cultures were grown at 30°C in SDM,H,W. For UV-survival curves dilutions of overnight cultures were spread on SDM,H,W plates and irradiated under a germicidal lamp (emitting primarily at 254 nm) at various doses (measured with a Spectroline DM-254N short wave ultraviolet meter; Spectronics Corporation, Westbury, NY) before incubation at 30°C in the dark. Colonies were counted after 2.5 days and percent survival was calculated.

For repair experiments a total of 2.5×10^9 cells at early stationary phase were transferred to a 50 ml centrifuge tube (Corning, NY) and pelleted (two tubes or 5×10^9 cells/time point). Cells were washed once and then suspended in 50 ml sterile water and allowed to incubate for 1 h to halt cell replication (35). The cells were then poured into sterile glass Petri dishes (to a depth of ~1.5 mm) and irradiated at 25 J/m^2 before being transferred back to 50 ml tubes and incubated in the dark for the indicated times.

Isolation of plasmid TRURAP

For experiments involving TRURAP the plasmid DNA was isolated as described (35), with the following modifications: 3 M potassium acetate, pH 4.8, was used instead of sodium acetate to precipitate the protein–SDS complexes and neutralize the pH following alkaline lysis of cells; the supercoiled plasmid was electroeluted from 1% agarose using a Centricon-30 filter in a Centrilutor apparatus (Amicon, Beverly, MA); the DNA was precipitated in the presence of 20 μg/ml mussel glycogen (Boehringer Mannheim Corp., Indianapolis, IN) before being dissolved in TE buffer (10 mM Tris, pH 8, 1 mM EDTA).

Isolation of genomic DNA

For genomic repair experiments cells were washed and incubated in the presence of zymolyase to form spheroplasts as described (35). Spheroplasts were lysed by resuspension in 1% SDS, 50 mM Tris–HCl, pH 8.0, 50 mM EDTA and incubated on ice for 20 min. The lysate was then extracted twice with phenol:chloroform:isoamyl alcohol (25:24:1) and once with chloroform:isoamyl alcohol (24:1) before RNA was digested with RNase Plus (4 μl/sample; 5 Prime → 3 Prime, Boulder, CO) at 30°C for 1 h. A 1/10 vol of 3 M sodium acetate was added and the genomic DNA precipitated with 2 vol. ethanol. The DNA was collected on a Pasteur pipette hook and dissolved in TE. It was precipitated again and the supernatant was removed. The DNA was washed with 80% ethanol and dried briefly at 50°C before being dissolved in TE.

Form I to Form II analysis of plasmid DNA

This analysis was done as described (4) with the following modifications: absorbance readings from the negative were obtained on a laser densitomer (LKB model 2222) and were transferred to computer disk via Gelscan XL and Gelcon programs (Pharmacia LKB). The programs MS Excel (Microsoft, Redmond, WA) and SigmaPlot for Windows (Jandel Scientific, San Rafael, CA) were used for data analysis. T4 endonuclease V was kindly provided by Dr R.Stephen Lloyd (University of Texas, Galveston, TX).

Alkaline gel analysis of genomic DNA

To analyze repair in genomic DNA an assay first developed by Sutherland and co-workers (36,37) was used. Figure 2 shows a schematic for these experiments. Approximately 15 μg of isolated total genomic DNA was treated (+) or not (–) with T4 endonuclease V as described (35). The samples were electrophoresed through a 0.8% alkaline agarose gel (38) for 16 h at 35 V (with buffer circulation) at room temperature. The gel was neutralized and stained as described (38). Photographs of the gel were taken as described (35), with the additional use of a yellow filter (Eastman Kodak Company). A strip of plastic impregnated with a fluorescent dye with an emission spectrum similar to ethidium bromide (peak emission at 576 nm; unpublished results) lying under a photographic steptablet filter (Eastman Kodak Company) was included in the photograph (see Fig. 5D). The filter had 21 steps ranging from 0.05 to 3.05 OD (step size 0.15 ± 0.02 OD). The photographic negative was scanned and data were transferred to computer as described above. In addition to the lanes containing samples and marker, an empty lane and the image of the step filter (see Fig. 5D) were also scanned.

In order to calibrate each film for accurate measurement of the amount of DNA present the film response function (a ninth order polynomial) for each negative was determined using the average apparent absorbance for each step of the steptablet filter image. This polynomial was used to convert the apparent absorbance values to real absorbance values for the densitometer scans from the gel. Two separate backgrounds were then subtracted from the data lanes (39). The first background was contributed by the gel itself. This was removed by subtracting the absorbance values determined for the empty lanes from the values of the data lanes. The second background is visible as a smear running most of the length of the gel in each of the (–) lanes (see Fig. 5). This smear is generated from random nicks introduced into the DNA during isolation and must be removed to obtain an accurate measure of damage remaining in each sample. This was removed by subtracting the broad shallow peak defined by the smear of DNA below the large molecular weight DNA in each (–) lane from both that lane and its paired (+) lane. This is equivalent to 'peak deconvolution' and accounts for a smear below a peak of interest (see 39).

The area under the corrected scans was determined as a running total using the trapezoidal rule (40). The data point corresponding to half that area (x_{med}) was obtained. Using a standard curve generated from the marker lane each x_{med} was then converted to L_{med}, the median length in bases. The median length was then converted to the number average molecular length, $\bar{L}_n$, using the following equation (36):

$$\bar{L}_n = 0.6L_{med} \quad 1$$

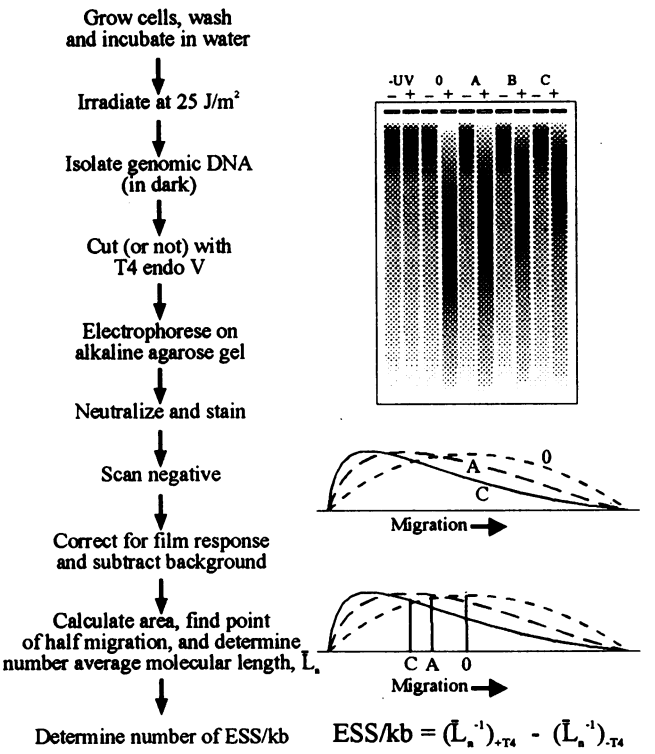

Figure 2. Experimental scheme for genomic repair analysis. The gel representation shows a stained alkaline gel from samples treated (+) or not (–) with T4 endonuclease V. A–C indicate repair times. Shading indicates intensity of staining and thus amount of DNA. Curved lines under the gel representation indicate densitometer scans of the T4 endonuclease V-treated lanes from 0, A and C. Repair is seen as a shift in the peak density of the scan to slower migrating positions of the gel. The 'drop lines' in the second set of curves indicate positions of x_{med} for those three lanes (see Materials and Methods).

Finally, the number of CPDs (expressed as enzyme-sensitive sites/kb; *ESS*/kb) was calculated (36):

$$ESS = \bar{L}_n^{-1}(+\text{T4 endonuclease V}) - \bar{L}_n^{-1}(-\text{T4 endonuclease V}) \quad 2$$

Site-specific repair analysis of plasmid DNA

Isolated supercoiled plasmid TRURAP DNA, prepared as described above, was digested with restriction enzyme (either *Eco*RI or *Xba*I; Gibco-BRL, Gaithersburg, MD), then digested with T4 endonuclease V and electrophoresed through a 1.5% alkaline agarose gel (38) for 16 h at 35 V, as described (4). DNA was transferred to Hybond-N+ membrane (Amersham Corporation, Arlington Heights, IL) in 0.4 N NaOH. The membrane was washed once with water and once with 2× SSC (0.3 M NaCl, 20 mM sodium citrate, pH 7.0) and dried overnight.

Radioactive strand-specific RNA probes were synthesized from plasmid pSTPEX, which contains the *Eco*RI–*Xba*I fragment of TRURAP (see Fig. 1), as described (4). Membranes were pre-hybridized and hybridized at 42°C as directed by Promega (41). A volume containing 3–5 × 10^6 c.p.m. was added to 3 ml pre-hybridization buffer and exposed to the membrane overnight at 42°C in a roller bottle and hybridization oven (Robbins Scientific, Sunnyvale, CA). The membrane was washed at 42°C as directed by Promega before being exposed to pre-flashed

X-ray film (Hyperfilm-MP; Amersham) with an intensifying screen.

The autoradiogram was photographed by a Kodak solid-state CCD camera and analyzed on a Visage 60 computer using Whole Band Analysis software (Bio Image, Ann Arbor, MI). The integrated intensity of the bands in the –UV lane was subtracted from the corresponding bands in the sample lanes as a background correction and to correct for random nicking. The band intensities within a lane were normalized to a particular band in the *ARS1* region (see Fig. 1), previously determined to be unrepaired (4), to correct for loading differences between lanes. Each band in the repair lanes was then divided by the corresponding band in the no repair lane and the common logarithm of this fraction was plotted versus time (4) (see Fig. 8A). The slope of a linear fit to the data yields the pseudo first order rate constant for the repair of that particular site (4).

RESULTS

We constructed a *rad7*Δ mutant strain to be isogenic to our wild-type strain. With this strain the repair characteristics were investigated in both plasmid and genomic DNA. The repair assays used involved the CPD-specific enzyme T4 endonuclease V (4,35), which makes a single strand nick at the site of any unrepaired CPDs (42).

UV survival and damage levels

Figure 3 shows the survival characteristics of the various strains. At the dose used in the repair experiments (25 J/m^2) ~80% of the wild-type cells were able to grow on selective plates, while only ~0.2% of the *rad7*Δ cells were able to grow. Comparison of these survival curves with several other reports (22,25,26,43) indicates there are large variations between different *rad7*Δ strains. Survival of our *rad7*Δ mutant at 50 J/m^2 is almost four orders of magnitude lower than that of Miller *et al.* (22) or Verhage *et al.* (26). Two possible explanations for these differences are: (i) differences in the UV meters used; (ii) differences in genetic backgrounds of the strains. Furthermore, only two of these studies (26,43) were with mutants isogenic to the corresponding wild-type strain. Perhaps a more informative way of reporting UV-survival curves would be to report survival as a function of lesions induced/unit length DNA.

At a dose of 25 J/m^2 an average of 1.2 ± 0.2 CPD/plasmid (2.6 kb) were induced into TRURAP in all three strains (*rad7*Δ, *rad1*Δ and wild-type). In genomic DNA the amount of damage induced at that dose was 1.2 ± 0.3 CPD/5.2 kb single-stranded DNA (i.e. the same amount of DNA as in TRURAP) in all three strains. These dimer yields indicate that there is no inherent difference between genomic and plasmid DNA in the yield of CPDs.

Whole plasmid repair in TRURAP

To examine the overall repair characteristics of the plasmid the resistance of supercoiled (Form I) plasmid DNA, cutting by T4 endonuclease V was used as an assay for the average number of CPD/plasmid following different repair times (35). As shown in Figure 4A, the wild-type strain shows an increase in the amount of DNA in the Form I band and a concurrent loss of DNA in the Form II band as repair time progresses (Fig. 4A, +T4 endonuclease V lanes). The mutant *rad1*Δ strain shows no such change

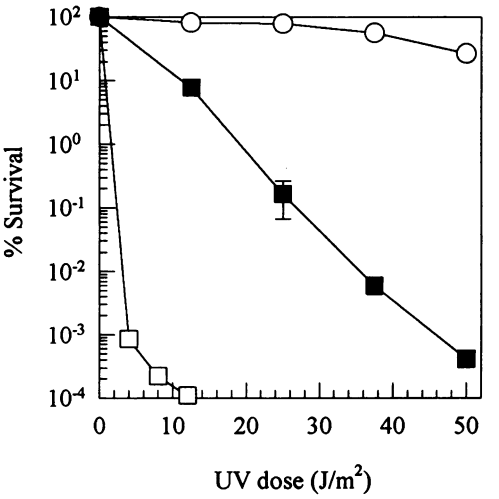

Figure 3. UV–survival curves of yeast strains. Cells were grown, spread on plates and irradiated at 12.5, 25, 37.5 or 50 J/m^2 as described (Materials and Methods). Colonies were counted after 2.5 days at 30°C and percent survival calculated. Error bars indicate standard error from three separate experiments, where the average count of three plates was taken. Symbols are: ○, FTY23 (wild-type); ■, JMY6-7 (*rad7*Δ); □, JMY1-1 (*rad1*Δ).

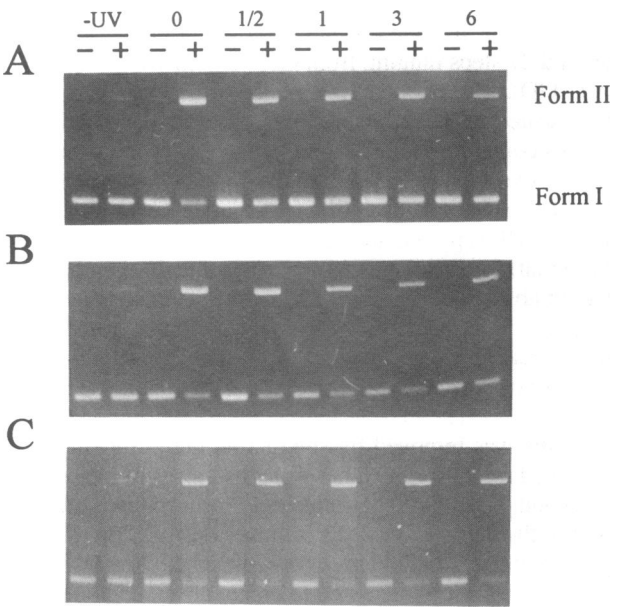

Figure 4. Whole plasmid repair gels. Shown are gels of the entire TRURAP plasmid isolated from cells irradiated at 25 J/m^2 and allowed to repair for various times. Plasmid was either treated (+) or not treated (–) with T4 endonuclease V. (**A**) FTY23 (wild-type). (**B**) JMY6-7 (*rad7*Δ). (**C**) JMY1-1 (*rad1*Δ).

in the amounts of DNA in the two bands (Fig. 4C), while the *rad7*Δ strain shows an intermediate level of change (Fig. 4B).

When quantified (Materials and Methods), the amount of repair in the plasmid for the *rad7*Δ strain levels off to ~45% after 6 h (Fig. 6, solid circles). The *rad1*Δ mutant shows no repair (Fig. 6, solid diamonds), while wild-type shows nearly complete repair (>85%) after this time period (Fig. 6, solid squares).

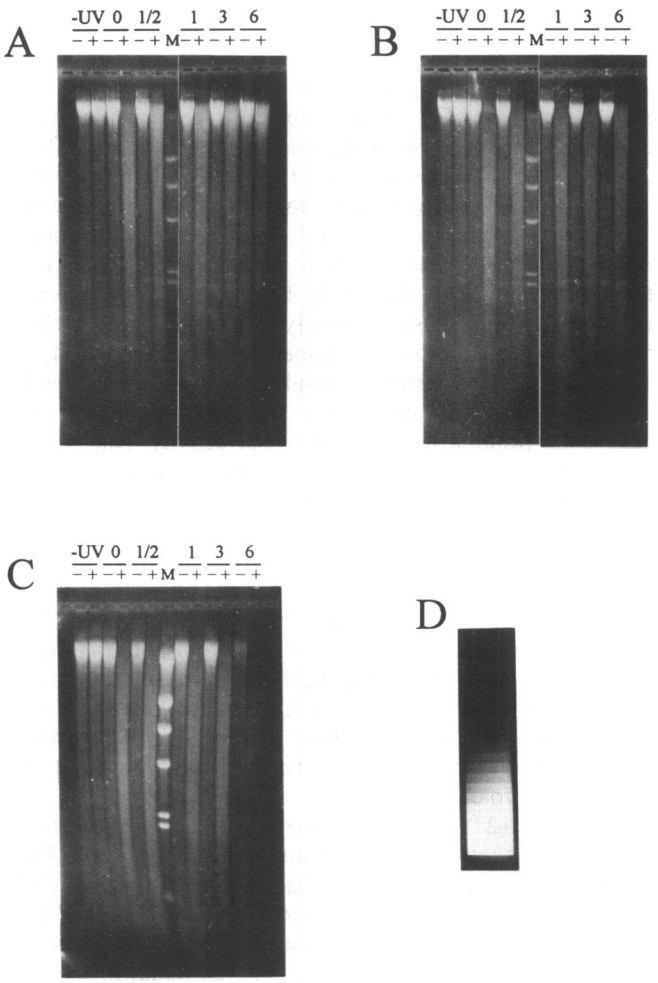

Figure 5. Genomic repair gels. Shown are stained alkaline agarose gels of genomic DNA isolated from cells irradiated as in Figure 4 and treated (+) or not treated (–) with T4 endonuclease V. (**A**) FTY23 (wild-type). (**B**) JMY6-7 (*rad7*Δ). (**C**) JMY1-1 (*rad1*Δ). (**D**) A sample image of a step filter used to calibrate the photographic negative (Materials and Methods). Marker (M) is λ DNA digested with *Hin*dIII.

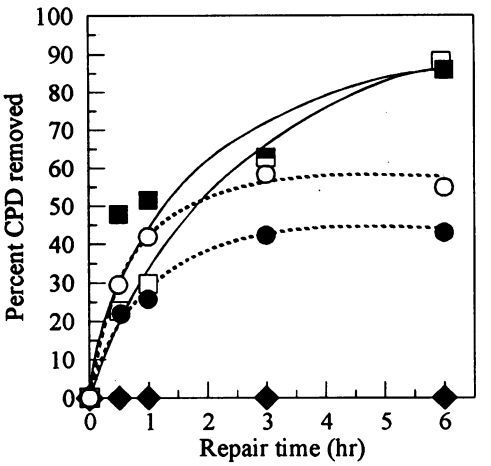

Figure 6. Repair curves of genomic and TRURAP DNA in three strains. Shown are the averages of three independent experiments (except for *rad7*Δ genomic) for genomic (□) and plasmid TRURAP (■) DNA in FTY23 (wild-type), genomic (○; average of two independent experiments) and plasmid TRURAP (●) DNA in JMY6-7 (*rad7*Δ) and both genomic and plasmid DNA (◆) in JMY1-1 (*rad1*Δ). Standard deviations for plasmid repair experiments ranged from ±17% for the 30 min time points to ±5% for the 6 h time points. Standard deviations for genomic repair experiments ranged from ±25% for the 30 min time point to ±8% for the 6 h time point.

Genomic repair

To determine if the time course of repair observed in the plasmid reflected that in the genome, repair of CPDs in genomic DNA was studied. The number average molecular length of genomic DNA before and after T4 endonuclease V treatment was used to calculate the average number of CPD/kb (see Fig. 2 and Materials and Methods). A shift in the average mobility of DNA after T4 endonuclease V treatment toward larger molecular weights indicates repair (Fig. 2 and Materials and Methods).

For the *rad7*Δ mutant, the amount of DNA shift does not approach that observed for wild-type, but is there, nonetheless, indicating repair is occurring (compare Fig. 5B with Fig. 5A and C, especially the 6+ lanes). When photographic negatives of the gels were scanned and the scans quantified we observed that repair of CPDs in genomic DNA leveled off to ~55% in 6 h (Fig. 6, open circles). In contrast, ~90% of the CPDs are removed from genomic DNA in wild-type cells during this time (Fig. 6, open squares). As with the plasmid DNA, the *rad1*Δ mutant strain showed no repair of genomic DNA (Fig. 6, solid diamonds).

Site-specific repair in plasmid TRURAP

In order to examine the repair of CPDs induced in TRURAP at a higher resolution, a site-specific analysis was used (4). In this assay supercoiled plasmid is gel purified and cut with both a restriction enzyme (*Eco*RI or *Xba*I) and T4 endonuclease V before electrophoresis through an alkaline agarose gel. After transferring the DNA to a membrane, it is hybridized with a short strand-specific probe to one end of the cut plasmid (4). The resulting autoradiograms for DNA from the *rad7*Δ mutant (Fig. 7) show that certain bands disappear as time progresses, especially along the transcribed strand of the *URA3* gene (SP6-generated RNA probe). This is the case in both the *Eco*RI cut samples (Fig. 7, top left) and the *Xba*I cut samples (Fig. 7, lower left). Across the same regions probed with T7-generated RNA (Fig. 7, right panels) bands disappear at a much slower rate, indicating that the non-transcribed strand of the *URA3* gene is not repaired efficiently, if at all. Other transcriptionally active regions of TRURAP (see Fig. 1) are also repaired. For instance, in the gels probed with T7-RNA, above the 186 base marker (*Xba*I) or above the 1569 base marker (*Eco*RI) bands disappear. These bands correspond to regions transcribed within the so-called 'UNF' nucleosomes (see Fig. 1). The same experiments were performed with the wild-type strain and the resulting autoradiograms were similar to those reported previously (4) for this strain (data not shown).

Figure 8A shows an example of the decrease in relative band intensity for a particular site (760 base band from Fig. 7, *Eco*RI/SP6, arrowhead) for the wild-type and the *rad7*Δ mutant strains. The points represent the log of the percent of DNA remaining (compared with no repair) for that band. The slopes of

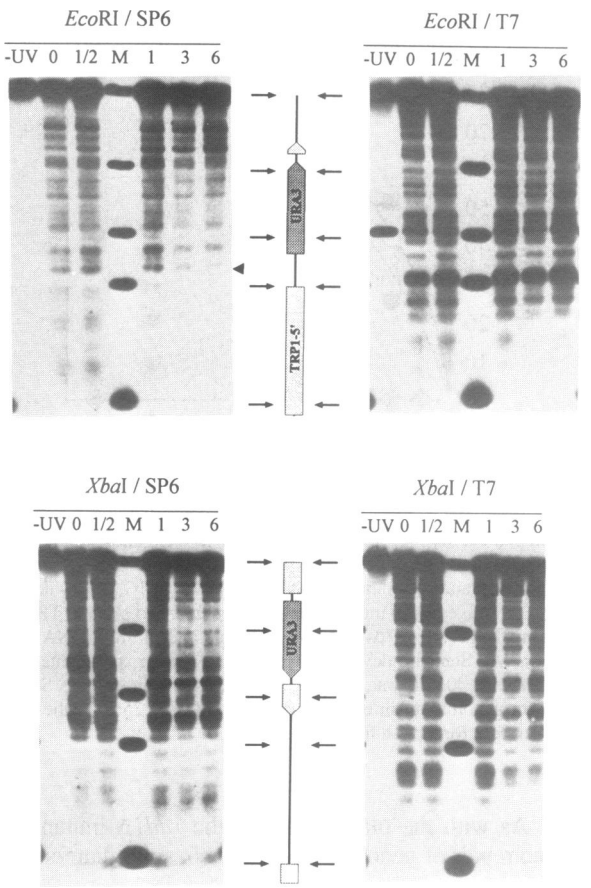

Figure 7. Site-specific repair gels. Isolated TRURAP (see Fig. 4 legend) was cut and electrophoresed on alkaline agarose gels as described (Materials and Methods). Shown are the four site-specific repair gels for JMY6-7 (*rad7Δ*). In between each pair of gels is an abbreviated map of TRURAP. The horizontal arrows indicate the position of the marker bands (M) along the map. Marker sizes are 2619, 1576, 938, 615 and 186 bases (top to bottom). The band near the 938 base marker in the –UV lane of the *Eco*RI/T7 gel is a partial *Eco*RI digestion product and was not included in the quantitation. The arrowhead between the *Eco*RI/SP6 gel and the map of TRURAP, above the 615 base marker, is the CPD site used for Figure 8A.

the linear regressions are the apparent first order rate constants for repair at that site (see Materials and Methods for details).

The repair rate constants for 44 different CPD sites in TRURAP for the *rad7Δ* mutant strain are shown by the open circles and dashed lines in Figure 8B (transcribed strand on top, relative to *URA3*, non-transcribed strand on bottom). The regions of efficient repair (high rate constant) in the *rad7Δ* strain correspond to transcribed regions of the plasmid. However, at most sites the rate of repair in the *rad7Δ* strain was less than that observed for wild-type (closed circles and solid lines). Neither the rate nor the location of repair seemed to be influenced by the presence or absence of nucleosomes (Fig. 8B). Repair was clearly observed at some sites (777, 1370 and 1536 bases) in the non-transcribed strand of *URA3* in wild-type cells and was diminished at these same sites in the *rad7Δ* strain (Fig. 8B). Furthermore, in both strains low repair occurs in both strands of DNA near the replication origin (*ARS1*), in agreement with previous results (4). Taken together these results imply that there is an overall decrease in repair efficiency of CPDs in the *rad7Δ* mutant.

DISCUSSION

The results of the whole plasmid repair and genomic repair assays indicate that the *rad7Δ* mutant is partially deficient in overall nucleotide excision repair or in repair of a subclass of CPDs. In agreement with previous reports (21–23,25) we find that *RAD7* is not an essential gene for excision repair of all CPDs, since some repair is observed. Even though not all of the CPDs are removed (Figs 4, 5 and 7), the cells survive at an intermediate level to that of wild-type and *rad1Δ* (Fig. 3). In the case of the *rad1Δ* mutant even a low level of CPDs is extremely lethal (Fig. 3) and no CPDs are repaired (Figs 4 and 5), in agreement with past reports (44,45).

Using a well-characterized plasmid (29,30) we investigated the rate and location of repair sites and correlated these with nucleosome position and transcriptional activity. Nucleosome position appeared to have no effect on repair of the plasmid in the *rad7Δ* mutant, indicating that the Rad7 protein does not function to remove nucleosomes from damaged DNA. However, transcriptional activity seemed to be very important for the repair of CPDs. Those CPDs not repaired by the *rad7Δ* strain lie primarily within the non-transcribed strand of transcribed areas (e.g. *URA3*, bottom panel of Fig. 8B) and in the ~300 bp non-transcribed region near the *ARS1* site (both panels of Fig. 8B). In addition, we observed a lower rate of repair at most sites repaired by the mutant (Fig. 8B). This indicates that the Rad7 protein is involved in repair of both non-transcribed and transcribed regions of DNA and may have a general role in NER.

Waters *et al.* (27) propose that Rad7 plays a role in rendering non-transcribed regions of the genome accessible to repair. They base this on their finding that pre-irradiation of cells at a low UV dose, waiting 1 h and then irradiating the cells at a higher UV dose does not increase repair of the non-transcribed *HMLα* locus in their *rad7Δ* strain. This pre-irradiation was found to increase repair of the transcribed *MATα* locus. However, they observe that pre-irradiation does increase repair of both the *MATα* and *HMLα* loci in wild-type cells. A concern with this report is that the experiments were done with actively growing cells and repair was conducted in growth media. Under these conditions replication will be detected as repair (unless newly replicated DNA is removed before the repair assay) and the survival of *rad* mutant strains is considerably less than wild-type strains (for example see Fig. 3). When cells are arrested in water much less cell death occurs (i.e. 'liquid holding'; 46).

Our finding that primarily the transcribed regions of TRURAP are repaired in *rad7Δ* cells agrees with Waters *et al.* (27). Most (~65%) of the TRURAP plasmid is transcribed (see Fig. 1) and the only non-transcribed *double-stranded* region is the ~300 bp around the *TRP1-3'* and *ARS1* sequences (Fig. 1) (30). Of the six sites observed on both strands lying in that region all are repaired more slowly in *rad7Δ* cells compared with wild-type (Fig. 8B). This observation seems to indicate that the *RAD7* gene product is involved in making non-transcribed regions accessible to repair enzymes, in agreement with Waters *et al.* (27). However, we also observe lower repair rates at most sites in the transcribed regions, indicating that the Rad7 protein may have a more global role in NER (see below).

Verhage *et al.* (26) reported that the *rad7Δ* mutant does not repair the non-transcribed *HMLα* locus, but does repair the transcribed *MATα* locus. They also reported that the mutant does not repair ~30% of genomic DNA (using antibodies to detect cyclobutyl thymine dimers). They further reported that the

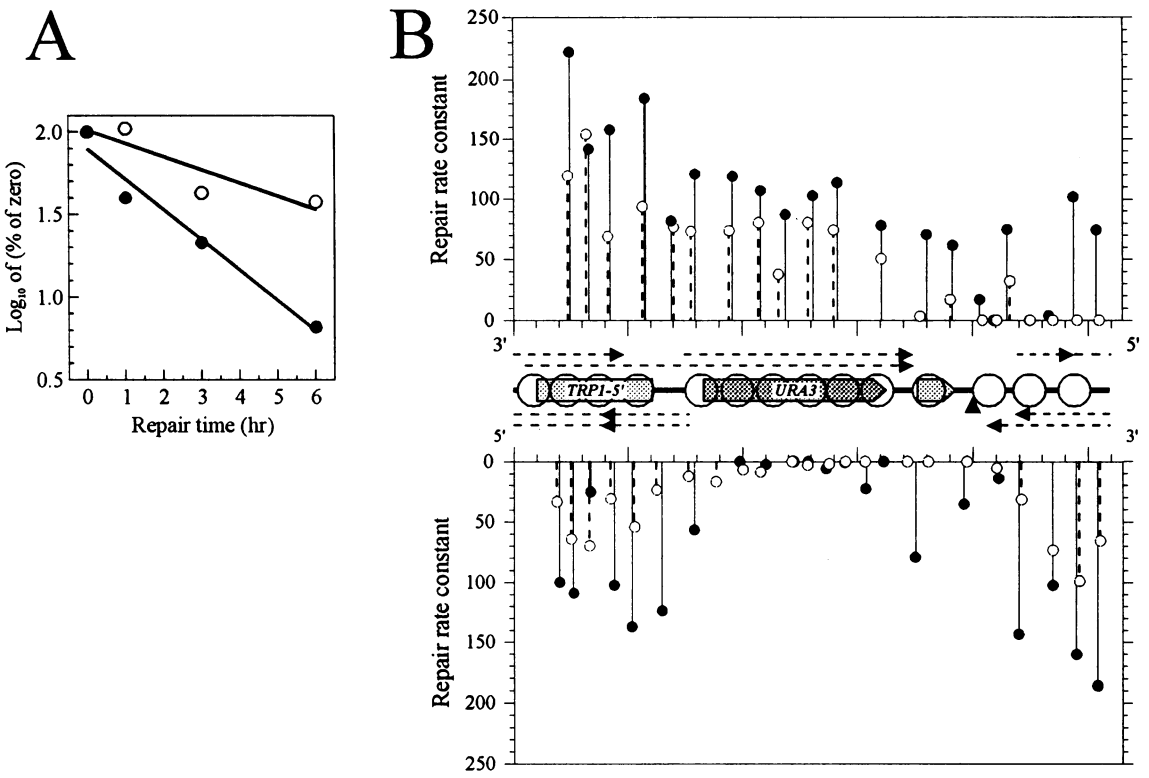

Figure 8. Site-specific repair map for TRURAP. (**A**) Log_{10} of the percentage of corrected intensity of the no repair sample plotted versus repair time for the 760 base band from the *Eco*RI/SP6 gel of Figure 7 (*rad7*Δ) and wild-type (gel not shown). Lines are for linear regressions of the data in each case. Symbols are: ●, FTY23 (wild-type); ○, JMY6-7 (*rad7*Δ). (**B**) First order rate constants for repair at various sites within TRURAP. The transcribed strand, relative to *URA3* (probed with SP6-RNA), is shown on the top (3′→5′) and the non-transcribed strand (probed with T7-RNA) is shown on the bottom (5′→3′). Averages were taken between *Eco*RI and *Xba*I generated data and between closely spaced bands. Solid bars and closed circles are from FTY23 (wild-type), dashed bars and open circles are from JMY6-7 (*rad7*Δ). Between the two panels is a linear map of TRURAP showing nucleosome positions (circles), transcripts (dashed-line arrows), gene locations (shaded boxes) and the *ARS1* consensus sequence (solid arrowhead). Major tick marks on the abscissa are 500 bases apart, starting at the *Eco*RI restriction site.

mutant did not repair the non-transcribed strand of the *RPB2* gene, but did repair the transcribed strand. Our results for repair of sites within the *URA3* gene in TRURAP agree. However, these authors report that their *rad7*Δ strain repairs the transcribed strand at the *same rate and to the same extent* as their wild-type strain (26). This differs from our findings that the rate of repair in our *rad7*Δ strain is less than in wild-type at most CPD sites within the transcribed strand of *URA3*, as well as other transcribed regions of TRURAP (Fig. 8B). This could reflect an additional role of Rad7 in NER, possibly in assembly of the NER complex (28).

The observed differences between our results and those of Verhage *et al.* (26) could be explained by the different genetic backgrounds in the two strains. A major difference between these *rad7*Δ mutant strains is their UV survival. At a dose of 50 J/m^2, the survival of their strain (MGSC104) is ~3% (26), while that of our strain (JMY6-7) is much lower (Fig. 3). Others (25,43) have observed survival levels for *rad7* mutants closer to what we observe. This indicates that the genetic background of the MGSC104 strain may have a profound effect on survival and, presumably, repair in that strain.

The differences between this report and that of Verhage *et al.* (26) might also be explained by different experimental techniques. Their repair experiments were conducted on growing cells and the repair incubation was conducted in growth media, while our experiments were conducted on cells growth arrested in water (as discussed earlier). Finally, the differences might be explained by the fact that the rates we measured were for a yeast plasmid folded into chromatin, not chromosomal DNA. However, Sweder and Hanawalt (5) have shown that both plasmid and chromosomal copies of a gene (*RPB2*) are repaired at the same rate and to the same extent, indicating that plasmid DNA accurately reflects what occurs in at least some regions of chromosomal DNA. We note, however, that Sweder and Hanawalt (5) conducted their study in a wild-type background and their observations may not be reflected in *rad* mutants.

The loss of repair in the double-stranded non-transcribed region near the *ARS1* site of TRURAP (Fig. 8B) indicates that the Rad7 protein plays a role in repair of non-transcribed regions, in agreement with earlier reports (26,27). In addition, the apparent loss of repair at several sites in the non-transcribed strand of *URA3*, in comparison with the already low rate of repair in wild-type cells (Fig. 8B, lower panel), indicates that the Rad7 protein participates in repair of the non-transcribed strand of active genes, as observed previously (26). Based on these data, the role of the Rad7 protein could be in: (i) recognizing damage in non-transcribed DNA; (ii) recruiting repair enzymes to non-transcribed strands; (iii) making non-transcribed regions accessible to repair enzymes. The last proposed role is supported by several reports (26,27,43). However, as mentioned above, the decreased repair rates observed at most sites in TRURAP for the

rad7Δ mutant (Fig. 8B) indicates that the Rad7 protein is involved in more than the repair of non-transcribed regions of DNA.

ACKNOWLEDGEMENTS

We thank Dr Louise Prakash for supplying plasmid pR7.2 and Dr R. Stephen Lloyd for supplying the enzyme T4 endonuclease V. We also thank members of the Smerdon laboratory for their stimulating and critical discussions of this work. This study was supported by NIH grant ES02614 from the National Institute of Environmental Health Sciences.

REFERENCES

1 Modrich,P. (1994) *Science*, **266**, 1959–1960.
2 Sancar,A. (1994) *Science*, **266**, 1954–1956.
3 Mellon,I., Spivak,G. and Hanawalt,P.C. (1987) *Cell*, **51**, 241–249.
4 Smerdon,M.J. and Thoma,F. (1990) *Cell*, **61**, 675–684.
5 Sweder,K.S. and Hanawalt,P.C. (1992) *Proc. Natl. Acad. Sci. USA*, **89**, 10696–10700.
6 Mellon,I. and Hanawalt,P.C. (1989) *Nature*, **342**, 95–98.
7 Selby,C.P. and Sancar,A. (1993) *Science*, **260**, 53–58.
8 van Gool,A.J., Verhage,R., Swagemakers,S.M.A., van de Putte,P., Brouwer,J., Troelstra,C., Bootsma,D. and Hoeijmakers,J.H.J. (1994) *EMBO J.*, **13**, 5361–5369.
9 Bailly,V., Sommers,C.H., Sung,P., Prakash,L. and Prakash,S. (1992) *Proc. Natl. Acad. Sci. USA*, **89**, 8273–8277.
10 Bardwell,A.J., Bardwell,L., Johnson,D.K. and Friedberg,E.C. (1993) *Mol. Microbiol.*, **8**, 1177–1188.
11 Sung,P., Reynolds,P., Prakash,L. and Prakash,S. (1993) *J. Biol. Chem.*, **268**, 26391–26399.
12 Habraken,Y., Sung,P., Prakash,L. and Prakash,S. (1993) *Nature*, **366**, 365–368.
13 Feaver,W.J., Svejstrup,J.Q., Bardwell,L., Bardwell,A.J., Buratowski,S., Gulyas,K.D., Donahue,T.F., Friedberg,E.C. and Kornberg,R.D. (1993) *Cell*, **75**, 1379–1387.
14 Guzder,S.N., Sung,P., Bailly,V., Prakash,L. and Prakash,S. (1994) *Nature*, **369**, 578–581.
15 Sung, P., Prakash, L., Weber, S. and Prakash, S. (1987) *Proc. Natl. Acad. Sci. USA*, **84**, 6045–6049.
16 Sung, P., Prakash, L., Matson, S.W. and Prakash, S. (1987) *Proc. Natl. Acad. Sci. USA*, **84**, 8951–8955.
17 Naegeli,H., Bardwell,L. and Friedberg,E.C. (1992) *J. Biol. Chem.*, **267**, 392–398.
18 Naegeli,H., Bardwell,L. and Friedberg,E.C. (1993) *Biochemistry*, **32**, 613–621.
19 Sung,P., Watkins,J.F., Prakash,L. and Prakash,S. (1994) *J. Biol. Chem.*, **269**, 8303–8308.
20 Guzder,S.N., Sung,P., Prakash,L. and Prakash,S. (1993) *Proc. Natl. Acad. Sci. USA*, **90**, 5433–5437.
21 Prakash,L. and Prakash,S. (1979) *Mol. Gen. Genet.*, **176**, 351–359.
22 Miller,R.D., Prakash,L. and Prakash,S. (1982) *Mol. Gen. Genet.*, **188**, 235–239.
23 White,C.I. and Sedgwick,S.G. (1985) *Mol. Gen. Genet.*, **201**, 99–106.
24 Jones,J.S., Prakash,L. and Prakash,S. (1990) *Nucleic Acids Res.*, **18**, 3281–3285.
25 Perozzi,G. and Prakash,S. (1986) *Mol. Cell. Biol.*, **6**, 1497–1507.
26 Verhage,R., Zeeman,A.-M., de Groot,N., Gleig,F., Bang,D.d., van de Putte,P. and Brouwer,J. (1994) *Mol. Cell. Biol.*, **14**, 6135–6142.
27 Waters,R., Zhang,R. and Jones,N.J. (1993) *Mol. Gen. Genet.*, **239**, 28–32.
28 Prakash,S., Sung,P. and Prakash,L. (1993) *Annu. Rev. Genet.*, **27**, 33–70.
29 Thoma,F. (1986) *J. Mol. Biol.*, **190**, 177–190.
30 Bedoyan,J., Gupta,R., Thoma,F. and Smerdon,M.J. (1992) *J. Biol. Chem.*, **267**, 5996–6005.
31 Ausubel,F.M., Brent,R., Kingston,R.E., Moore,D.D., Seidman,J.G., Smith,J.A. and Struhl,K. (1989) *Current Protocols in Molecular Biology*. John Wiley & Sons, New York, NY.
32 Ito,H., Murata,K. and Kimura,A. (1984) *Agric. Biol. Chem.*, **48**, 341–347.
33 Gietz,R.D. and Schiestl,R.H. (1991) *Yeast*, **7**, 253–263.
34 Boeke,J.D., LaCroute,F. and Fink,G.R. (1984) *Mol. Gen. Genet.*, **197**, 345–346.
35 Smerdon,M.J., Bedoyan,J. and Thoma,F. (1990) *Nucleic Acids Res.*, **18**, 2045–2051.
36 Freeman,S.E., Blackett,A.D., Monteleone,D.C., Setlow,R.B., Sutherland,B.M. and Sutherland,J.C. (1986) *Anal. Biochem.*, **158**, 119–129.
37 Sutherland,B.M. and Shih,A.G. (1983) *Biochemistry*, **22**, 745–749.
38 Maniatis,T., Fritsch,E.F. and Sambrook,J. (1982) *Molecular Cloning: A Laboratory Manual*. Cold Spring Harbor Laboratory Press, Cold Spring Harbor, NY.
39 Mueller,J.P. (1994) Repair of plasmid and genomic DNA in two radiation sensitive mutants of *Saccharomyces cerevisiae*. PhD dissertation, Washington State University, Pullman, WA.
40 Thomas,G.B.,Jr and Finney,R.L. (1984) *Calculus and Analytical Geometry*. Addison-Wesley Publishing Company, Reading, MA.
41 Promega Corporaion (1993) *Transcription In Vitro Systems Technical Manual*. Promega Corporation, Madison, WI.
42 Dodson,M.L., Schrock,R.D. and Lloyd,S.R. (1993) *Biochemistry*, **32**, 8284–8290.
43 Paetkau,D.W., Riese,J.A., MacMorran,W.S., Woods,R.A. and Gietz,R.D. (1994) *Genes Dev.*, **8**, 2035–2045.
44 Reynolds,R.J. and Friedberg,E.C. (1981) *J. Bacteriol.*, **146**, 692–704.
45 Wilcox,D.R. and Prakash,L. (1981) *J. Bacteriol.*, **148**, 618–623.
46 Haynes,R.H. and Kunz,B.A. (1981) In Strathern,J.N., Jones,E.W. and Broach,J.R., (eds), *The Molecular Biology of the Yeast Saccharomyces: Life Cycle and Inheritance*. Cold Spring Harbor Laboratory Press, Cold Spring Harbor, NY, pp. 371–414.
47 Bajwa,W., Torchia,T.E. and Hopper,J.E. (1988) *Mol. Cell. Biol.*, **8**, 3439–3447.